First results from the far-infrared polarimeter system on the Madison Symmetric Torus reversed field pinch

N. E. Lanier,[a] J. K. Anderson, C. B. Forest, and D. Holly
Department of Physics, University of Wisconsin-Madison, Madison, Wisconsin 53706

Y. Jiang and D. L. Brower
Department of Electrical Engineering, University of California at Los Angeles, Los Angeles, California 90095

(Presented on 9 June 1998)

The far-infrared laser interferometer on the Madison Symmetric Torus has recently been upgraded to allow simultaneous interferometry and polarimetry measurements. Centered around a heterodyne laser system that operates at $\lambda \simeq 432\ \mu$m, the diagnostic has a frequency response of 1 kHz for the polarimeter and up to 1 MHz for the interferometer. The distribution of laser power through the 11 chord system is managed with wire mesh beamsplitters. Concurrent with the system upgrade to polarimetry, a detailed study of the effect of the wire mesh beamsplitters on beam polarization was conducted. The study shows that the mesh characteristics must be included to extract the polarimetry phase measurement from the raw data. The modifications to the data analysis as well as preliminary five chord polarimetry profile data are presented. © *1999 American Institute of Physics.*
[S0034-6748(99)52901-8]

I. INTRODUCTION

Internal measurements of the poloidal field allow us to deduce the toroidal current density and are of vital interest to the MST ($R_0 = 1.5m$, $a = 0.52m$) reverse field pinch (RFP).[1] When coupled with the information gathered from other magnetic diagnostics, polarimetry measurements aid in accurately reconstructing the full toroidal magnetic equilibrium. Once the equilibrium is known, important quantities like the stored energy, the pressure profile, and especially λ $(= J \cdot B/B^2)$ can be obtained.

The polarimetry technique employed on the Madison Symmetric Torus (MST) is the same as first described by Rice,[2] where a rotating elliptically polarized beam is created by a spinning $\lambda/2$ wave plate. Passing the beam through a polarizer yields an amplitude-modulated beam; the phase of the amplitude modulation with respect to a reference allows measurement of the Faraday rotation due to the plasma. This technique has successfully been implemented on both Microwave Tokamak Experiment (MTX)[3] and TEXT-U[4] tokamaks.

However, to implement this system on MST (Fig. 1), some modifications were necessary. The RFP's requirement of a close fitting conducting wall for external kink stability and the use of image currents in the shell as a substitute for external vertical field coils, placed severe limitations on the far-infrared (FIR) beam accessibility. Previous polarimetry systems of this type used large parabolic mirrors to distribute the FIR beam through the plasma. On MST, an access port this large is unacceptable due to associated field errors, so a system with 11 discrete chords was chosen.

To divide the laser power among the 11 chords, wire mesh beamsplitters are used. The meshes are electroformed from a nickel substrate by Buckbee/Mears[5] and are commercially available in many wire densities. Wire mesh beamsplitters complicate the polarimetry measurement because their anisotropic reflective/transmission[6,7] properties can distort the polarization state of the beam. However, these distortions are systematic and specific to each mesh type making it possible to characterize and remove the errors introduced by these components.

II. POLARIZATION INTEGRITY

The most important aspect in making an accurate polarimeter is maintaining the polarization integrity throughout the system. Since only one component of the polarization ellipse is measured, deformations in the polarization state will appear as phase shifts. If the contamination is serious enough, the measured phase can become discontinuous and highly erratic. Considerable effort has been committed to identifying and correcting aspects of the system that were destructive to the beam polarization.

The entrance and exit ports to the tank were a major concern. The requirement for small holes (38 mm diameter) in the thick conducting shell (5 cm) meant that the beam would have to navigate narrow tubes as it passed through the tank. Beam expansion, small errors in alignment, and refraction effects from the plasma made reflections off the inner walls of the tubes unavoidable. Threaded inserts,[8] with 20 and 48 threads per inch (TPI) were installed to minimize any contamination from these reflections. Further modifications included the installation of two large slot windows in the vacuum duct and wherever possible shortening the entrance tubes. With these modifications, tests indicate that beam propagation through the tank in vacuum introduces no measurable polarization contamination.

[a]Electronic mail: lanier@loki-physics.wisc.edu

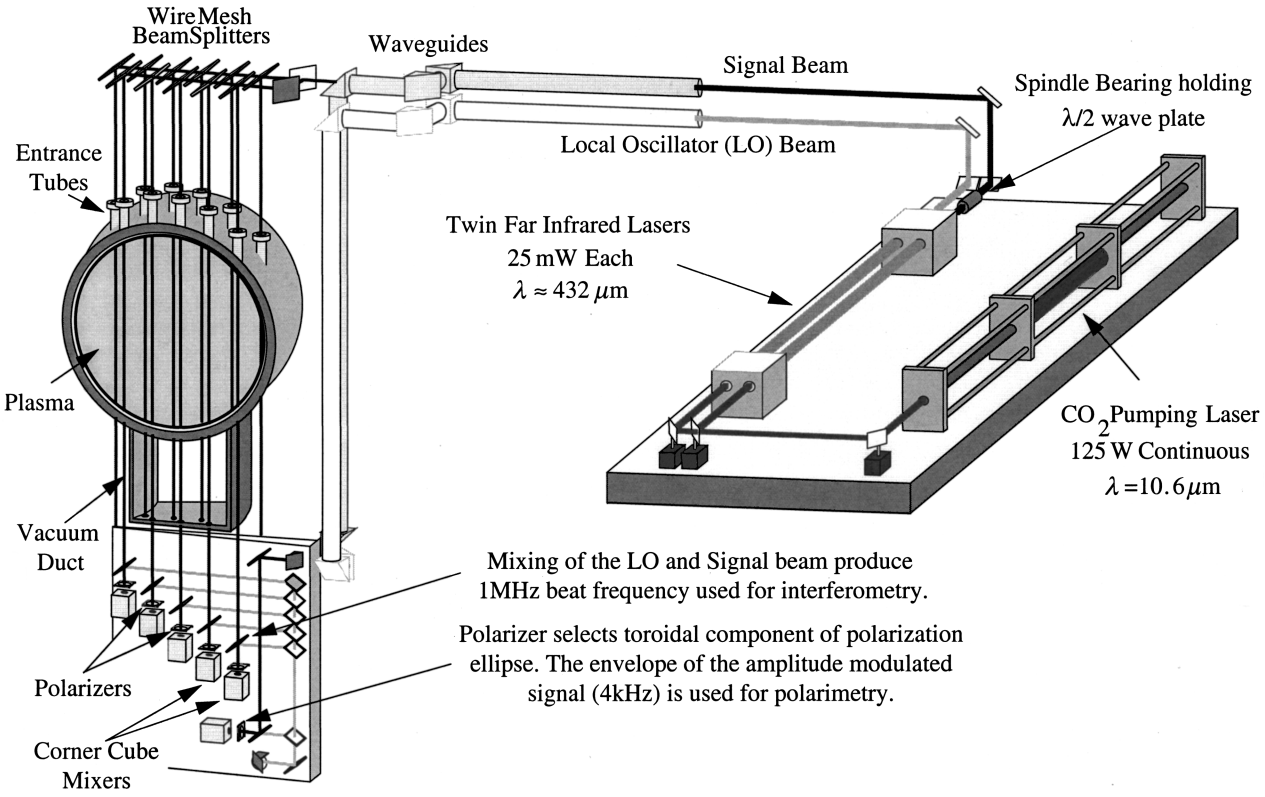

FIG. 1. The far-infrared laser interferometry/polarimetry system.

Another important issue is that of feedback. Reflections of stray laser power back into the laser cavity can seriously degrade the stability of the laser. The dominant sources of feedback in the system are the wave plates, polarizers, and mixers. To combat this problem, small incident angles were introduced for all components so that the reflections would not propagate back through the system. To further minimize the feedback, polarizers were placed on the output end of the laser cavity. These modifications along with strategically placed microwave absorber eliminated most of the feedback sources.

The last major issue deals with the polarization properties of the wire mesh beamsplitters in the system. The polarimeter system was designed to be insensitive to amplitude changes in the beam; any deformations in the polarization state near the spindle bearing or after the vacuum vessel will appear as an additional fixed offset in the measured polarimetery phase. However, modifications to the polarization state between where the reference beam is split off and the plasma will couple multiplicatively to the measured phase of each chord. This coupling will be explored in greater detail in Sec. III.

III. DERIVATION OF THE MESH COUPLING

At these wavelengths, the wire mesh beamsplitters, unlike silvered mirrors, have anisotropic reflective and transmission properties. These anisotropies are dependent on both mesh geometry and orientation and have the effect of modifying the polarization of the beam. Since the polarimeter is indiscriminant in measuring polarization changes in the beam, a useful measurement requires that the contributions from the meshes and the plasma be decoupled.

To understand how anisotropic reflection/transmission affects the measured polarimetry signal, we expound on the example outlined in Fig. 2 where two wire mesh beamsplitters are used to distribute the beam between the signal and reference legs. In keeping with convention, we define the transverse electric (TE) polarization component such that its electric field vector oscillates parallel to the axis of rotation of the mesh. Hence the transverse magnetic (TM) polarization is the electric field component orthogonal to TE. All polarizations incident on the mesh can be described as some linear combination of TE and TM.

A. Modeling the beam polarization

The beam out of the laser is linearly polarized and then elliptized with a λ/4 plate. The elliptization is necessary for

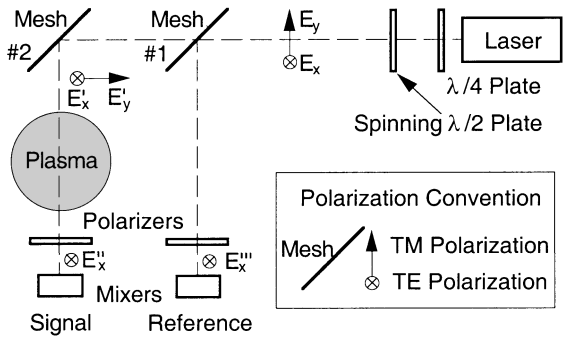

FIG. 2. Hypothetical setup to examine the effects of wire mesh beamsplitters on measured Faraday rotation.

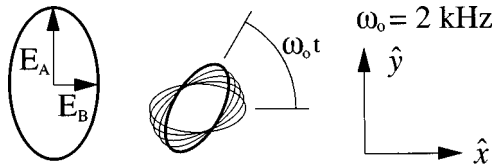

FIG. 3. The beam polarization can be modeled as an ellipse with major (E_A) and minor (E_B) radii rotating at ω_0.

the simultaneous operation of the interferometer and polarimeter. The spinning λ/2 wave plate then rotates the ellipse.

The fast dynamics (1 MHz) are not important for the polarimeter discussion. The polarimeter measures the modulation of one component of the 2 kHz rotating ellipse. Using the coordinates described in Fig. 3 we model the ellipse as follows.

$$\text{TE wave} \Rightarrow E_x = E_A \cos(\omega_0 t) + E_B \sin(\omega_0 t),$$

$$\text{TM wave} \Rightarrow E_y = E_A \sin(\omega_0 t) - E_B \cos(\omega_0 t).$$

Rewriting the TE and TM components into complex notation we have

$$E_x = \gamma \exp(+i\omega_0 t) + \gamma^* \exp(-i\omega_0 t),$$

$$E_y = -i\gamma \exp(+i\omega_0 t) + i\gamma^* \exp(-i\omega_0 t),$$

where $\gamma = (E_A - iE_B)/2$.

B. Polarization change via reflection/transmission

To accurately simulate the reflective/transmissive properties of the meshes, four new terms are introduced. T_{TE}, T_{TM}, R_{TE}, R_{TM} are the transmissivities and reflectivities of the TE and TM modes, respectively. Before the beam in the signal leg can reach the plasma, it must first propagate through Mesh No. 1 and then reflect off of Mesh No. 2 introducing the following distortion in its electric field components:

$$E_x' = (T_{\mathrm{TE1}})(R_{\mathrm{TE2}})E_x \quad E_y' = (T_{\mathrm{TM1}})(R_{\mathrm{TM2}})E_y.$$

C. Faraday rotation and polarization selection

As the signal beam propagates through the plasma a Faraday rotation δ is imparted to the polarization ellipse. δ is proportional to the line integrated product of the component of the magnetic field parallel to the beam propagation and the electron density and is the quantity we wish to measure. Finally, a polarizer selects the toroidal component of the beam making the electric field incident on the detector

$$\begin{aligned} E_{\mathrm{Sig}} &= E_x' \cos\delta + E_y' \sin\delta \\ &= T_{\mathrm{TE1}}R_{\mathrm{TE2}}E_x \cos\delta + T_{\mathrm{TM1}}R_{\mathrm{TM2}}E_y \sin\delta \\ &= \eta\gamma \exp(+i\omega_0 t) + \eta^*\gamma^* \exp(-i\omega_0 t), \end{aligned}$$

where $\eta = T_{\mathrm{TE1}}R_{\mathrm{TE2}} \cos\delta - iT_{\mathrm{TM1}}R_{\mathrm{TM2}} \sin\delta$.

When extracted from the measured power, the amplitude modulated envelope has the form

$$\begin{aligned} P_{\mathrm{SigEnv}} = {} & \eta\gamma\eta\gamma \exp(+2i\omega_0 t) + 2\eta\gamma\eta^*\gamma^* \\ & + \eta^*\gamma^*\eta^*\gamma^* \exp(-2i\omega_0 t). \end{aligned}$$

Similarly it can be shown that the reference envelope is described by

$$\begin{aligned} P_{\mathrm{RefEnv}} = {} & -(R_{\mathrm{TE1}})^2[\gamma\gamma \exp(+2i\omega_0 t) \\ & + 2\gamma\gamma^* - \gamma^*\gamma^* \exp(-2i\omega_0 t)]. \end{aligned}$$

The phase difference between these signals is proportional to the Faraday rotation angle.

D. Digital phase comparison

As with the interferometer, the polarimetry phase comparison is evaluated digitally in a manner similar to that outlined by Jiang.[9] The resulting measured phase Δ is

$$\tan\Delta = \frac{-2T_{\mathrm{TE1}}R_{\mathrm{TE2}}T_{\mathrm{TM1}}R_{\mathrm{TM2}} \cos\delta \sin\delta}{(T_{\mathrm{TE1}}R_{\mathrm{TE2}} \cos\delta)^2 + (T_{\mathrm{TM1}}R_{\mathrm{TM2}} \sin\delta)^2}.$$

The typical Faraday rotation angles for MST plasmas are $\delta \approx 0.15$ rad and the TM/TE ratios of the meshes are of order unity. Noting that $(T_{\mathrm{TM1}}R_{\mathrm{TM2}}/T_{\mathrm{TE1}}R_{\mathrm{TE2}})^2 \tan^2\delta \ll 1$, the equation for $\tan\Delta$ can be expanded to yield

$$\begin{aligned} \tan\Delta = {} & -2\tan\delta\left(\frac{T_{\mathrm{TM1}}R_{\mathrm{TM2}}}{T_{\mathrm{TE1}}R_{\mathrm{TE2}}}\right) \\ & \times\left[1 + \left(\frac{T_{\mathrm{TM1}}R_{\mathrm{TM2}}}{T_{\mathrm{TE1}}R_{\mathrm{TE2}}}\right)^2 \tan^2\delta + O(\tan^4\delta)\right]. \end{aligned}$$

Since $\Delta, \delta \rightarrow$ small, our equation to lowest order, becomes

$$\Delta \cong -2\delta\left(\frac{R_{\mathrm{TM2}}}{R_{\mathrm{TE2}}}\right)\left(\frac{T_{\mathrm{TM1}}}{T_{\mathrm{TE1}}}\right). \tag{1}$$

In similar fashion it can be shown for the n mesh case that

$$\Delta \cong -2\delta\left(\frac{R_{\mathrm{TM}}}{R_{\mathrm{TE}}}\right)_n \prod_{i=1}^{n-1}\left(\frac{T_{\mathrm{TM}}}{T_{\mathrm{TE}}}\right)_i. \tag{2}$$

The plasma induced rotation (δ) becomes

$$\delta \cong -\frac{\Delta}{2\Upsilon}, \tag{3}$$

where we have defined a mesh correction factor (Υ) to be

$$\Upsilon = \left(\frac{R_{\mathrm{TM}}}{R_{\mathrm{TE}}}\right)_n \prod_{i=1}^{n-1}\left(\frac{T_{\mathrm{TM}}}{T_{\mathrm{TE}}}\right)_i. \tag{4}$$

TABLE I. Summary of the mesh types used along with the measured mesh correction factors. Errors in Υ vary from 4% to 75%.

Chord	$R - R_0$ (cm)	x/a	Mesh (LPI)	Υ	Error
*P*36	+36	+0.69	50	1.24	±0.05
*P*21	+21	+0.40	90.1	0.95	±0.04
*P*06	+06	+0.12	125	0.72	±0.04
*N*09	−17	−0.17	150	1.26	±0.05
*N*24	−24	−0.46	Mirror	2.07	±0.07

IV. CHARACTERIZATION OF THE MESHES

Both transmissivity and reflectivity ratios were measured for each mesh with the setup outlined in Fig. 4. The mesh

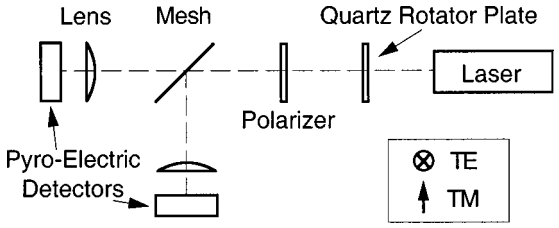

FIG. 4. Mesh characterization setup.

beamsplitter was set at an incident angle of 45°, as present in the polarimeter system. A slide mount that allowed easy removal and replacement without loss of alignment was used to hold the mesh. The quartz rotator plate and the polarizer could be adjusted to achieve the desired polarization incident on the mesh and pyroelectric detectors were used to measure the laser power. With this arrangement, transmission measurements could be made by simply removing the mesh. Characterizing the reflectance required exchanging the mesh with a mirror.

Tests were conducted for 12 meshes with line densities varying from 45 to 200 lines per inch (LPI). Some meshes (70 and 100 LPI) had resonances that made them unsuitable for use. Meshes with the most favorable characterics had line densities of 50, 125, and 150 LPI. The 90.1 LPI mesh was also acceptable although slightly lossy.

The question of polarization degradation resulting from the transmission through many meshes was also explored. Transmission measurements with up to six of the favorable meshes were conducted. No measurable degradation was present indicating that any adverse diffraction effects are small.

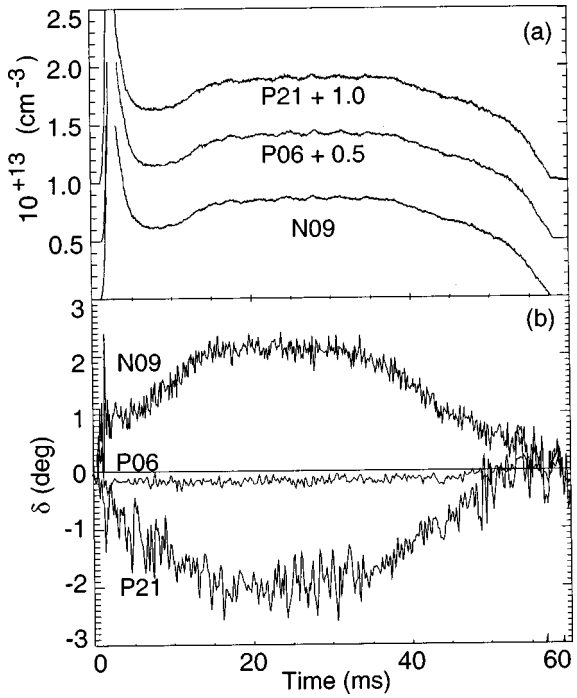

FIG. 5. (a) Line averaged electron density for the N09, P06, and P21 chords. (b) Measured Faraday rotation for the N09, P06, and P21 chords.

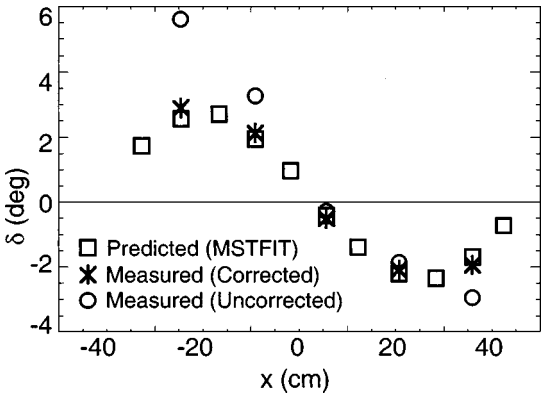

FIG. 6. Comparison between the five chord polarimetry data (corrected and uncorrected) and the data as predicted by the MSTFIT equilibrium reconstruction code.

Table I outlines the measured correction factors (Υ) for the five chords used in this experiment.

V. POLARIMETRY RESULTS AND DISCUSSION

For the initial tests, the system was run with five chords acquiring simultaneous electron density and poloidal magnetic field data. Shots were conducted at the moderate plasma parameters of $I_p \approx 275$ kA and $n_{e0} \approx 1.1\times 10^{13}$ cm^{-3}. Figure 5 shows the line averaged electron density and the Faraday rotation angle for chords N09, P06 and P21 during the shot. Both the corrected and uncorrected Faraday rotation profiles are shown in Fig. 6 along with the predicted Faraday rotation data via the MSTFIT[10] equilibrium reconstruction code. The results indicate clearly that when the correction factor Υ is applied, the FIR polarimeter results are in excellent agreement with the expectations from equilibrium reconstruction.

VI. SUMMARY

The modifications to the interferometer/polarimeter system have been very effective in improving its polarization integrity. An investigation of the wire meshes has shown that their anisotropic transmission/reflective properties affect the Faraday rotation measurement by distorting the polarization state of the laser beam. This effect is systematic in nature and when the meshes are properly characterized, the resulting contamination of the Faraday rotation measurement can be removed.

[1] R. N. Dexter, D. W. Kerst, T. W. Lovell, S. C. Prager, and J. C. Sprott, Fusion Technol. **19**, 131 (1991).
[2] B. W. Rice, Rev. Sci. Instrum. **63**, 5002 (1992).
[3] B. W. Rice, Ph.D. thesis, University of California-Davis, California 1992, UCLR-LR-111863.
[4] D. L. Brower, L. Zeng, and Y. Jiang, Rev. Sci. Instrum. **68**, 419 (1997).
[5] Buckbee/Mears Inc., St. Paul, MN.
[6] C. C. Chen, IEEE Trans. Microwave Theory Tech. **MTT-9**, 627 (1970).
[7] Y. S. Hwang and H. K. Park, Appl. Opt. **28**, 4999 (1989).
[8] R. M. Erickson, Los Alamos Internal Report, 1985, LA-10731-T.
[9] Y. Jiang, D. L. Brower, L. Zeng, and J. Howard, Rev. Sci. Instrum. **68**, 902 (1997).
[10] C. B. Forest *et al.*, ''EFIT Equilibrium reconstructions for the MST reversed field pinch,'' APS poster, Annual Meeting of Division of Plasma Physics November 17–21, 1997, Pittsburgh PA.